MAJOR ARTICLE

Function of HAb18G/CD147 in Invasion of Host Cells by Severe Acute Respiratory Syndrome Coronavirus

Zhinan Chen,[1,a] Li Mi,[1,a] Jing Xu,[1,a] Jiyun Yu,[3] Xianhui Wang,[1] Jianli Jiang,[1] Jinliang Xing,[1] Peng Shang,[1] Airong Qian,[1] Yu Li,[1] Peter X. Shaw,[5] Jianwei Wang,[4] Shumin Duan,[4] Jin Ding,[2] Chunmei Fan,[2] Yang Zhang,[1] Yong Yang,[1] Xiaoling Yu,[1] Qiang Feng,[1] Biehu Li,[1] Xiying Yao,[1] Zheng Zhang,[1] Ling Li,[1] Xiaoping Xue,[1] and Ping Zhu[2]

[1]Department of Cell Biology, the Fourth Military Medical University, and [2]Department of Clinical Immunology, Xijing Hospital, the Fourth Military Medical University, Xi'an, and [3]Institute of Basic Medical Sciences, Academy of Military Medical Sciences, and [4]Institute of Viral Disease Control and Prevention, Chinese Center for Disease Control and Prevention, Beijing, China; [5]Department of Molecular Medicine, University of California, San Diego, San Diego

To identify the function of HAb18G/CD147 in invasion of host cells by severe acute respiratory syndrome (SARS) coronavirus (CoV), we analyzed the protein-protein interaction among HAb18G/CD147, cyclophilin A (CyPA), and SARS-CoV structural proteins by coimmunoprecipitation and surface plasmon resonance analysis. Although none of the SARS-CoV proteins was found to be directly bound to HAb18G/CD147, the nucleocapsid (N) protein of SARS-CoV was bound to CyPA, which interacted with HAb18G/CD147. Further research showed that HAb18G/CD147, a transmembrane molecule, was highly expressed on 293 cells and that CyPA was integrated with SARS-CoV. HAb18G/CD147–antagonistic peptide (AP)–9, an AP of HAb18G/CD147, had a high rate of binding to 293 cells and an inhibitory effect on SARS-CoV. These results show that HAb18G/CD147, mediated by CyPA bound to SARS-CoV N protein, plays a functional role in facilitating invasion of host cells by SARS-CoV. Our finding provide some evidence for the cytologic mechanism of invasion by SARS-CoV and provide a molecular basis for screening anti-SARS drugs.

Severe acute respiratory syndrome (SARS) coronavirus (CoV), the pathogen ascertained to be responsible for SARS, caused disastrous results around the world at the end of 2002 [1, 2]. How SARS-CoV infects host cells still remains unclear, and the results of studies of the other CoVs suggest that CoVs infect host cells by direct or indirect interaction between viral proteins and cellular proteins expressed on the unit membrane [2–5]. Cyclophilin A (CyPA) is a ubiquitously distributed cellular protein and is thought to assist protein folding and to function as a chaperone. It can be integrated with virions of some kinds of viruses, such as HIV-1 [6] and vaccinia virus [7]. By interacting with cellular receptors or through other pathways, integrated CyPA plays a role in viral invasion or replication. CD147 (called "EMMPRIN" in [8] and "basigin" in [9]) is a transmembrane glycoprotein and belongs to the immunoglobulin superfamily. It is a receptor for CyPA and contributes to viral infection or inflammatio [6, 10]. HAb18G/CD147, which was developed and was identifie to be a member of the CD147 family in our laboratory, is involved in tumor metastasis, inflamma tion, and virus infection [11–19]. Inspired by the known relationship between CD147 and HIV-1, we conducted the present study to investigate the possible function of HAb18G/CD147 in invasion of host cells by SARS-CoV.

MATERIALS AND METHODS

Viruses and cells. SARS-CoV (BJ04) and 293 cells (ATCC CRL-1573) were supplied by the Chinese Center

Received 15 June 2004; accepted 23 September 2004; electronically published 25 January 2005.

Financial support: National Natural Science Foundation of China (grant 39989002 to Z.C.); Hi-Tech Research and Development Program of China (grant 2001AA215061 to Z.C.).

[a] Z.C., L.M., and J. Xu contributed equally to this work.

Reprints or correspondence: Dr. Ping Zhu, Dept. of Clinical Immunology, Xijing Hospital, the Fourth Military Medical University, 17 Changlexi St., Xi'an, 710032, P. R. China (zhuping@fmmu.edu.cn).

The Journal of Infectious Diseases 2005;191:755–60

0022-1899/2005/19105-0017$15.00

for Disease Control and Prevention (China CDC). The cells were cultured in Dulbecco's MEM (Gibco BRL) containing 10% fetal calf serum (Gibco BRL).

Peptides. HAb18G/CD147–antagonistic peptide (AP)–9 (an AP of HAb18G/CD147 obtained in our laboratory, composed of 12 aa residues) [20–24], CB-2 (a randomly synthesized peptide also containing 12 aa residues, used as negative control), and biotin–AP-9 were synthesized by CL Bio-Scientific Their purity, assayed by high-pressure liquid chromatography, was >95%, and their amino-acid sequences and molecular weights, respectively, were as follows: AP-9, YKLPGHHHHYRP and 1541.09; CB-2, LHRHSHGHSYTS and 1389.50; and biotin–AP-9, biotin-YKLP-GHHHHYRP and 1767.69.

Coimmunoprecipitation (Co-IP) analysis. The ProFound mammalian Co-IP kit (Pierce) and the ECL Plus Western blotting detection system (Amersham Pharmacia) were used in accordance with the manufacturers' instructions. To analyze the interaction between HAb18G/CD147 and CyPA, 100 μg of HAb18G/CD147 (a recombinant extracellular fragment of HAb18G/CD147, prepared in our lab) was incubated with an equivalent amount of CyPA (Alexis Biochemical) overnight at room temperature (RT). The mixture was then added to the gel, which was coupled with 200 μg of mouse anti–human HAb18G/CD147 monoclonal antibody (MAb) HAb18 (prepared in our lab) [25–33], for incubation with gentle end-over-end mixing for 4 h. After the bound proteins were eluted, aliquots of the eluent were analyzed by a Western blot developed with rabbit anti–human CyPA antibody (diluted 1:2000; Calbiochem-Novabiochem) and horseradish peroxidase (HRP)–conjugated goat anti–rabbit IgG (diluted 1:5000; Amersham Pharmacia). Purchased CyPA (2.5 μg) was used as the positive control.

To analyze the interaction between CyPA and SARS-CoV structural proteins (spike [S], membrane [M], envelope [E], and nucleocapsid [N]; provided by China CDC), the gel was coupled with 200 μg of CyPA, which was used as the bait protein. Mouse antibodies to the 4 proteins (diluted 1:1000) and HRP-conjugated goat anti–mouse IgG (diluted 1:5000) were used in the subsequent Western blot analyses. Five micrograms of the respective protein was used as the positive control. Blank controls were established in accordance with the manufacturer's instructions.

BIAcore spectroscopy. Surface plasmon resonance analysis was performed, by use of a BIAcore X biosensor system (BIAcore), as described elsewhere [34]. HAb18G/CD147 or CyPA was immobilized on research-grade CM5 sensor chips (BIAcore), with a concentration of 100 μg/mL in 10 mmol/L sodium acetate (pH 6.0), by use of the amine coupling kit supplied by the manufacturer. Approximately 2000 resonance units of HAb18G/CD147 or CyPA was immobilized under these conditions. Unreacted moieties on the surface were blocked with ethanolamine, and the chips were measured in HEPES-buffered saline containing 10 mmol/L HEPES (pH 7.4).

Analyses were performed at 25°C, at a flo rate of 5 μL/min for determination of on-rates and equilibrium binding and 50 μL/min for determination of off-rates. To determine which protein of SARS-CoV could be captured by CyPA or HAb18G/CD147, the S, M, E, and N proteins of SARS-CoV were diluted to 1 μg/mL in HEPES-buffered saline for capture by the CyPA or HAb18G/CD147 surface. Surfaces were typically regenerated with 100 mmol/L hydrochloric acid and 0.2 mol/L Tris buffer.

To assess the affinit of N protein to CyPA, N protein was diluted to 40, 32, 24, 16, and 8 nmol/L for capture by the CyPA surface. Biosensor data were prepared for kinetic analysis, by zeroing the time and response before the firs injection. To correct refractive index changes and nonspecifi binding, the binding responses generated in the control experiments were subtracted from the responses generated in the CyPA–N protein interaction. The binding data were then globally fitte to the following reaction mechanism, in which CyPA and N protein are represented by A and B, respectively: $A + B \rightleftharpoons_{K_d} AB$. An equilibrium dissociation rate constant (K_d) was calculated from the kinetic rate constants by nonlinear fittin of the primary sensorgram data by use of BIAevaluation software (version 3.1; BIAcore).

Flow-cytometric analysis. 293 cells, at a density of 10^6 cells/mL, were incubated with either 10 μL of fluo escein isothiocyanate (FITC)–conjugated anti-CD147 antibody (Pharmingin) or 10 μL of FITC-conjugated mouse IgG1 (control; Pharmingin) in the dark for 30 min at 4°C. After being washed once with PBS, cells were fixe with 1% paraformaldehyde and analyzed by use of a FACSCalibur flo cytometer (Becton Dickinson) and CellQuest software (Becton Dickinson).

For analysis of AP-9 binding, the cells, blocked by goat serum for 30 min and incubated with biotin–AP-9 (fina concentration, 160 μg/mL) for 60 min, were washed and treated with 5 μL of avidin-FITC (Pharmingin) in the dark for 60 min at 4°C. Fixation and data analysis were performed as described above.

Confocal microscopy. 293 cells infected with SARS-CoV (BJ04) were cultured overnight on the sterilized cover slips and then washed in PBS and fixe with cold acetone for 30 min. For analysis of AP-9 binding, the cells were incubated with 25 μg of biotin–AP-9 and avidin-Cy3 (diluted 1:100; Sigma) in the dark overnight at 4°C. For analysis of blocking of AP-9, 25 μg of biotin–AP-9 was incubated with 2.5 μg of HAb18G/CD147 for 2 h at RT. Then, the mixture (biotin–Ap-9 and HAb18G/CD147) and avidin-Cy3 were added to the cells and incubated in the dark overnight at 4°C. The negative control, which was treated only with avidin-Cy3, was established at the same time. By use of the immuofluo escence double-staining method, the cells were incubated with 25 μg of HAb18 and an equivalent amount of biotin–AP-9 for 2 h at RT. After being washed with PBS, the cells were incubated with avidin-Cy3 (diluted 1:100) and FITC-labeled goat anti–mouse IgG (diluted 1:100; Wuhan BOSTER Bioengneer) in the dark overnight at 4°C. Careful observations

were made by use of a confocal microscope (IX-7; Olympus) with an object lens (UPLAPO; ×20 or ×40) and image-acquisition software (FLUOVIEW FV 300; Olympus).

Immunoelectronic microscopy. 293 cells infected with SARS-CoV (BJ04) were harvested and pelleted. The cells were treated with 4% glutaral for 30 min at 4°C and then were washed with phosphate buffer twice and treated with 1% osmium tetroxide (Polysciences) for 1.5 h at RT. After they had been dehydrated and embedded, the ultrathin sections of the cells were prepared.

The indirect gold colloid–labeling method was used to detect the localization of CyPA and HAb18G/CD147. After being washed in distilled water for 3 min, the ultrathin sections were treated with 1% H_2O_2 for 5 min and incubated with normal goat serum (diluted 1:75) for 10 min at RT and with rabbit anti–human CyPA antibody (diluted 1:25; Calbiochem-Novabiochem) or mouse anti–human CD147 antibody (diluted 1:50; Abcam) for 16 h at 4°C and for 1 h at RT. After being washed in PBS 3 times and in distilled water once, the sections were treated with PBS (containing 1% bovine serum albumin [BSA] [pH 8.2]) for 5 min and then were incubated with gold colloid–labeled protein A (diluted 1:50; diameter of the gold particle, 10 nm; prepared by the Academy of Military Medical Sciences [China]) for 1 h at RT and consecutively stained with 5% uranium acetate and lead acetate.

Then, the gold colloid double-labeling method was used to determine the colocalization of HAb18G/CD147 and AP-9. After being washed, the sections were treated with 1% H_2O_2 and normal goat serum (diluted 1:75), as described above. After being incubated with PBS (containing 1% BSA [pH 8.2]) for 5 min, the cells were incubated with the mixture of gold colloid–labeled AP-9 (diluted 1:400; diameter of the gold particle, 20 nm; prepared by the Academy of Military Medical Sciences [China]) and mouse anti–human CD147 antibody (diluted 1:50) and then were incubated with the gold colloid–labeled protein A (diluted 1:50) for 1 h at RT and were consecutively stained with 5% uranium acetate and lead acetate. Careful electronic microscopic observations were made by use of a JEM-100SX microscope (JEDL).

Analysis of cytopathic effect. 293 cells (4×10^5 cells/mL) were planted into 96-well plates (Costar) and kept in 5% CO_2 for 24 h at 37°C. For analysis of the toxicity of AP-9 to 293 cells, 2-fold dilution series of AP-9 (range, 3893.4–7.6 μmol/L), CB-2 (negative control; range, 4318.1–8.4 μmol/L), and gancyclovir (an antivirus chemical drug purchased from Hubei Keyi Pharmacy) injection (positive control; range, 23,508.2–45.8 μmol/L) were added to the cells. The TD_0 and TD_{50} were determined. For analysis of the virulence of SARS-CoV (BJ04) to 293 cells, viruses in 8 dilutions (10^{-1}–10^{-8}) were added to the cells, to determine the $TCID_{50}$ of SARS-CoV (BJ04). For the inhibitory-effect analysis of AP-9, the cells were incubated with 100 $TCID_{50}$ of SARS-CoV (BJ04) for 2 h. After the supernatant was discarded, 2-fold dilution series of TD_0 of AP-9 (range, 973.3–1.9 μmol/L), CB-2 (range, 359.8–0.7 μmol/L), and gancyclovir (range, 23,508.2–45.8 μmol/L) injection were added to the appropriate wells. Normal cell controls and virus controls were established. Cytopathic effects on the above cells were observed daily by use of an inverted microscope (XSZ-D; Nanjing Optical Instrument Factory of China) with an object lens (×10) and a camera (Ricon-5). Morphological changes observed in <25% of total cells were marked as "+", in 25%–50% were marked as "++", in 51%–75% were marked as "+++", and in 76%–100% were marked as "++++". TD_{50}, TD_0, $TCID_{50}$, IC_{50}, MIC, and treatment index (TI) were calculated by use of the Reed-Muench method. (For the inhibitory-effect analysis, when "+++" or "++++" was marked in virus control, the test was stopped.)

RESULTS

Interaction among N protein, CyPA, and HAb18G/CD147. Surface plasmon resonance analysis showed that none of the SARS-CoV S, M, E, or N proteins directly bound to HAb18G/CD147. However, N protein was found to interact with CyPA. In Co-IP analysis, when the mixture of HAb18G/CD147 and CyPA was added, CyPA was found to be indirectly bound to the gel, mediated by the specifi interaction of HAb18G/CD147 to its MAb, HAb18, which was used as the capture antibody. Thus, the HAb18-HAb18G/CD147-CyPA complex was formed. After the coimmunoprecipitated CyPA was eluted, it was visible by Western blot analysis performed with anti-CyPA antibody, which confi med the interaction between CyPA and HAb18G/CD147 (figu e 1*A*). Co-IP analysis further confi med the interaction between N protein and CyPA. Since CyPA was used as the bait protein, the coimmunoprecipitated N protein was visible by Western blot analysis performed with anti–N protein antibody (figu e 1*B*). The binding kinetics of N protein (in different concentrations) to CyPA was determined by surface plasmon resonance analysis, with a K_d of 0.04 μmol/L (figu e 1*C*).

Quantitative analysis of the expression of HAb18G/CD147 on SARS-CoV–permissive 293 cells and the binding of AP-9 to them. HAb18G/CD147 was found to be highly expressed on 293 cells, at the expression rate of 98.56% (figu e 2*A*). AP-9 was shown to be bound to the detected cells, at the binding rate of 98.15% (figu e 2*B*), which was very close to the expression rate of HAb18G/CD147 on the same kind of cells. AP-9 also had a median fluo escence intensity that was similar to that of HAb18G/CD147.

Cellular localization of HAb18G/CD147 and AP-9 on SARS-CoV–infected 293 cells. After being traced by fluo esceins, by use of laser scanning confocal microscopy, AP-9 was found to have high affinit to the detected cells. After incubation with HAb18G/CD147, the binding of AP-9 to the cells obviously

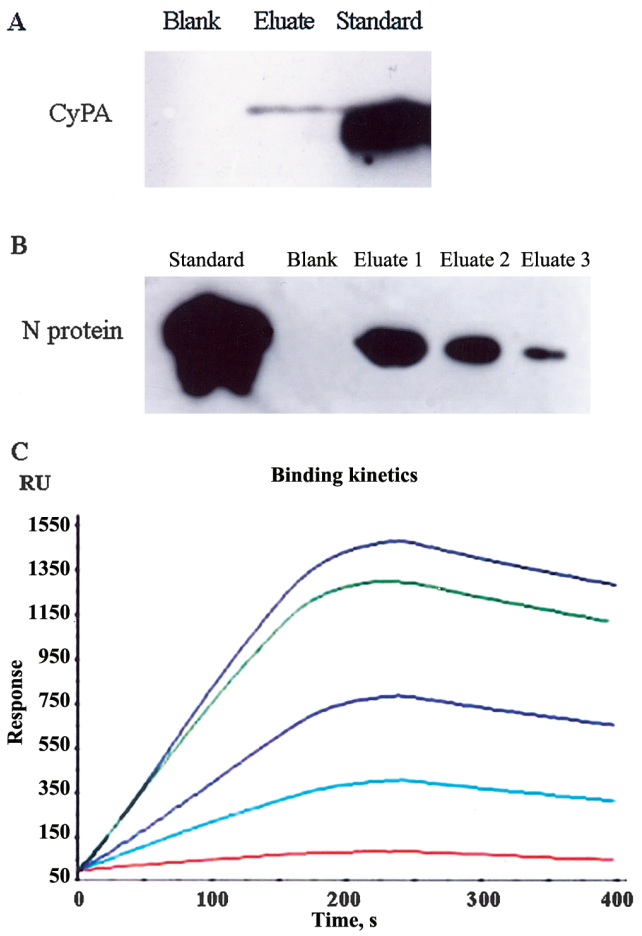

Figure 1. Analysis of protein-protein interaction. *A,* Coimmunoprecipitation (Co-IP) analysis–revealed interaction between HAb18G/CD147 and cyclophilin A (CyPA). Blank, blank control; eluate, coimmunoprecipitated CyPA in the eluate; standard, 2.5 μg of purchased CyPA. *B,* Co-IP analysis–revealed interaction between CyPA and severe acute respiratory syndrome coronavirus (SARS-CoV) nucleocapsid (N) protein. Blank, blank control; eluate 1, 2, and 3, coimmunoprecipitated N protein in orderly eluting; standard, 5 μg of N protein expressed in *Escherichia coli. C,* Binding kinetics of SARS-CoV N protein to CyPA, determined by surface plasmon resonance analysis. N protein, at different concentrations, could bind to CyPA. The lines with different colors are the binding kinetics curves of N protein to CyPA, at different concentrations: 40, 32, 24, 16, and 8 nmol/L. RU, resonance unit.

decreased (figu e 3*A*). By use of the immunofluo escence double-staining method, both HAb18G/CD147 and AP-9 were seen on the same binding sites (the cell membrane and the cytoplasm) of SARS-CoV–infected 293 cells (figu e 3*C*).

Subcellular localization of CyPA, HAb18G/CD147, and AP-9 on SARS-CoV–infected 293 cells. After being traced by gold colloid–labeled antibody, by use of electronic microscopy, CyPA was present on or around the surface of SARS-CoV (figu e 4*A*), indicating that CyPA was integrated with SARS-CoV. HAb18G/CD147 was located on the detected cell surface and the unit membrane, especially on the membrane of endoplasmic reticulum (ER) in cytoplasm (figu e 4*B*). The gold colloid double-labeling method was used, and the results showed that AP-9 was present on the same sites as was HAb18G/CD147 (figu e 4*C*).

Inhibitory effect of AP-9 on SARS-CoV. The results of analysis of cytopathic effect showed that AP-9, at a concentration of 973.3 μmol/L, was nontoxic to 293 cells—the TD_{50} and TD_0 for AP-9 were 1946.7 and 973.3 μmol/L, respectively. The $TCID_{50}$ of SARS-CoV to 293 cells was 10^{-3}. When 100 $TCID_{50}$ of SARS-CoV was added to the normally cultured 293 cells, the cells became infected and necrotic. After an MIC of AP-9 was added, the infected cells gradually recovered, whereas the AP-9–untreated virus control cells remained necrotic. The IC_{50}, MIC, and TI of AP-9 were 60.8 μmol/L, 30.4 μmol/L, and 32, respectively, whereas those of the positive control (with gancyclovir injection) were 91.8 μmol/L, 45.8 μmol/L, and 256, respectively; the TI of the negative control (with CB-2) was only 4.

DISCUSSION

It has been reported that CyPA can be specificall incorporated into the virions of HIV-1 and can significantl enhance an early step of cellular HIV-1 infection. CD147 can facilitate HIV-1 infection by interacting with virus-associated CyPA [6]. The present study has shown that HAb18G/CD147, a member of the CD147 family, can interact with CyPA, which may be associated with the SARS viruses and play a functional role in invasion of host cells by SARS-CoV. AP-9 has an inhibitory effect on SARS-CoVs.

SARS-CoV is known to have 4 structural proteins: S, M, E, and N. S, M, and E proteins are envelope proteins of SARS-CoV, and N protein is bound to viral RNA in the core. S protein of the other known CoVs is regarded to be responsible for both binding to receptors on host cells and membrane fusion [2]. In the present study, we have found that N protein may play a role in invasion of host cells by SARS-CoV. N protein was

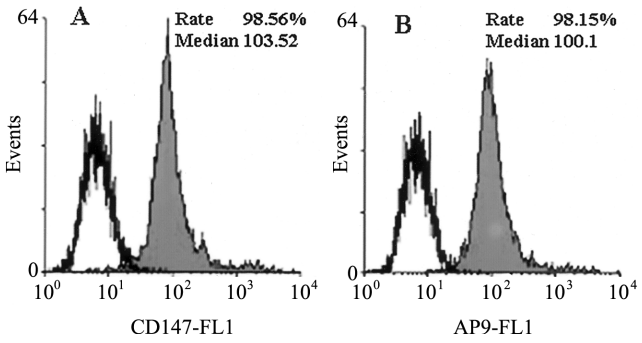

Figure 2. Flow-cytometric analysis of HAb18G/CD147 and antagonistic peptide (AP)–9. *A,* Expression of HAb18G/CD147 on 293 cells, analyzed by use of fluorescein isothiocyanate (FITC)–conjugated anti-CD147 antibody. *B,* Binding of AP-9 to 293 cells, analyzed by use of biotin–AP-9 and avidin-FITC.

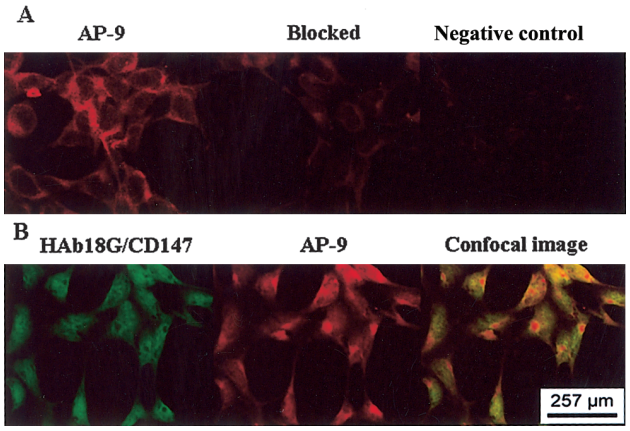

Figure 3. Confocal microscopic analysis of HAb18G/CD147 and antagonistic peptide (AP)–9. *A,* Severe acute respiratory syndrome coronavirus (SARS-CoV)–infected 293 cells stained with biotin–AP-9 and avidin-Cy3 *(red).* The result showed that AP-9 was bound to the detected cells. The binding of AP-9 to the detected cells was partially blocked by HAb18G/CD147. *B,* Immunofluorescence double-labeling method in SARS-CoV–infected 293 cells. Two kinds of fluorescence that indicated HAb18G/CD147 *(green)* and AP-9 *(red)* simultaneously presented in the cells, as observed by confocal imaging.

bound to CyPA, but S, M, and E proteins were not. However, CyPA was present only on the surface of mature SARS-CoVs, as observed by electronic microscopy. This findin seems to be contradictory to the findin that N protein locates in the core of the virus. This difference can be partly explained by the findin of a previous report that CyPA bound to viral proteins in the core can be relocated from the core to the viral surface during maturation of the virus [35]. The results of the present study also confi m the interaction between CyPA and HAb18G/CD147, as determined by Co-IP analysis, indicating that CyPA may act as a mediator between SARS-CoV N protein and HAb18G/CD147 in the process of invasion of host cells by SARS-CoV. By flow-cytometri analysis, confocal microscopy, and immunoelectronic microscopy, we found that HAb18G/CD147 was highly expressed in the SARS-CoV–permissive 293 cells and that it was located on the cytomembrane and the unit membrane in the cytoplasm (especially on the membrane of ER) as a transmembrane molecule. In the present study, the binding site of AP-9 was confi med to be on the HAb18G/CD147 molecule in the infected 293 cells, and AP-9 could efficientl block the binding sites of HAb18G/CD147 on the cytomembrane and the unit membrane in the cytoplasm of the 293 cells and had an inhibitory effect on SARS-CoV in vitro. From this finding we can conclude that HAb18G/CD147 is a functional molecule in SARS-CoV infection of host cells.

The mechanism of HAb18G/CD147 as a functional molecule can be inferred as follows: (1) CyPA is bound to N protein after invasion of host cells by SARS-CoV, and CyPA relocates to the virus surface during the maturation of the virus [35]; (2) the exposed CyPA molecules interact with HAb18G/CD147 on the cell membrane, which leads to the infection of other host cells; and (3) AP-9 blocks HAb18G/CD147, to prevent virus infection after those viruses complete their life cycle.

It also has been reported that the life cycle of CoVs that invade host cells includes N protein assembling with the full-length replicated RNA to form the RNA protein complex, which is associated with the M protein embedded in the membrane of ER and virus particles, which are formed as the nucleocapsid complex buds into ER [2, 36]. SARS-CoV is believed to have a similar process in the life cycle [36]. Therefore, we also inferred that SARS-CoV N protein associated with CyPA could interact with HAb18G/CD147 located on the membrane of ER and that the interaction could facilitate the virus particles in forming or budding into ER. AP-9, the small peptide, could enter the cells to prevent the virus particles from forming or budding into ER, by blocking HAb18G/CD147 located on ER. Thus, HAb18G/CD147 plays an important role in the process of invasion of host cells by SARS-CoV.

Both the function of HAb18G/CD147 in invasion of host cells by SARS-CoV and a clearer understanding of the mechanism responsible for the process need further confi mation.

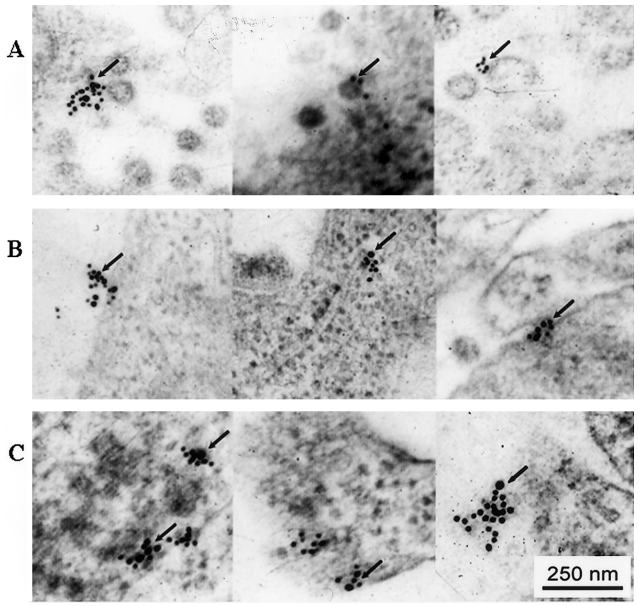

Figure 4. Subcellular localization of cyclophilin A (CyPA), HAb18G/CD147, and antagonistic peptide (AP)–9 on severe acute respiratory syndrome coronavirus (SARS-CoV)–infected 293 cells. *A,* Gold particles representing CyPA *(arrow),* located on the virus surface in a cluster or around the virus. *B,* Gold particles representing CD147 *(arrow),* located on the infected cell surface, across the membrane, or on the unit membrane in cytoplasm (especially on the membrane of endoplasmic reticulum) in cluster. *C,* Gold colloid double labeling. Gold colloid particles of 2 different sizes that indicated AP-9 (20 nm) and HAb18G/CD147 (10 nm), respectively, were located on the same site *(arrow).*

However, the present study may provide some evidence for the cytologic mechanism of invasion by SARS-CoV and may provide an important molecular basis for screening some anti-SARS drugs, such as antibody, polypeptide, immunocomplex, and small-molecule compounds.

Acknowledgments

We thank Dexing Li, Mifang Liang, Shengli Bi, Yinghua Chen, Hongwei Yang, Jian Liu, Bingfeng Wang, and Mei Huang, for their help in our experiments, and Yumei Zhou, Wenli Yan, and Fan Peng, for their careful reading of the manuscript.

References

1. Bloom BR. Lessons from SARS. Science **2003**; 300:701.
2. Rota PA, Oberste MS, Monroe SS. Characterization of a novel coronavirus associated with severe acute respiratory syndrome. Science **2003**; 300:1394–9.
3. Gallagher TM, Buchmeier MJ. Coronavirus spike proteins in viral entry and pathogenesis. Virology **2001**; 279:371–4.
4. Kontoyiannis DP, Pasqualini R, Arap W. Aminopeptidase N inhibitors and SARS. Lancet **2003**; 361:1558.
5. Krueger DK, Kelly SM, Lewicki DN. Variations in disparate regions of the murine coronavirus spike protein impact the initiation of membrane fusion. J Virol **2001**; 75:2792–802.
6. Pushkarsky T, Zybarth G, Dubrovsky L, et al. CD147 facilitates HIV-1 infection by interacting with virus-associated cyclophilin A. Proc Natl Acad Sci USA **2001**; 98:6360–5.
7. Castro AP, Carvalho TM, Moussatche N, Damaso CR. Redistribution of cyclophilin A to viral factories during vaccinia virus infection and its incorporation into mature particles. J Virol **2003**; 77:9052–68.
8. Biswas C, Zhang Y, DeCastro R, et al. The human tumor cell–derived collagenase stimulatory factor (renamed EMMPRIN) is a member of the immunoglobulin superfamily. Cancer Res **1995**; 55:434–9.
9. Miyauchi T, Kanekura T, Yamaoka A, Ozawa M, Miyazawa S, Muramatsu T. Basigin, a new, broadly distributed member of the immunoglobulin superfamily, has strong homology with both the immunoglobulin V domain and the β-chain of major histocompatibility complex class II antigen. J Biochem (Tokyo) **1990**; 107:316–23.
10. Yurchenko V, Zybarth G, O'Connor M, et al. Active site residues of cyclophilin A are crucial for its signaling activity via CD147. J Biol Chem **2002**; 277:22959–65.
11. Jiang JL, Yu MK, Chen ZN, Chan HC. cGMP-regulated store-operated calcium entry in human hepatoma cells. Cell Biol Int **2001**; 25:993–5.
12. Li Y, Shang P, Qian AR, Wang L, Yang Y, Chen ZN. Inhibitory effects of antisense RNA of HAb18G/CD147 on invasion of hepatocellular carcinoma cells in vitro. World J Gastroenterol **2003**; 9:2174–7.
13. Toole BP. Emmprin (CD147), a cell surface regulator of matrix metalloproteinase production and function. Curr Top Dev Biol **2003**; 54: 371–89.
14. Jiang JL, Zhou Q, Yu MK, Ho LS, Chen ZN, Chan HC. The involvement of HAb18G/CD147 in regulation of store-operated calcium entry and metastasis of human hepatoma cells. J Biol Chem **2001**; 276:46870–7.
15. Chen ZN, Yang Z, Mi L, Jiang JL, Guo XN. The structural and functional analysis of the hapetoma related factor, HAb18G. Chin J Cell Mol Immunol **1999**; 15:34.
16. Chen ZN, Li Y, Mi L. Gene cloning of CD147/HAb18G and study of its function in invasion and infiltratio of hepatoma. J Tumor Marker Oncol **2001**; 16:255–6.
17. Chen ZN. Antagonists of CD147 receptor target for SARS coronavirus and AIDS virus (HIV-1). Chinese patent CN1442203. May 15, 2003.
18. Jiang JL, Yao XY, Zhou J, Huang Y, Zhang Y, Chen ZN. HAb18G/CD147 stimulates MMPs release and activation via calcium mobilization in human hepatoma cells. J Tumor Marker Oncol **2003**; 18:299–310.
19. Chen ZN. Use of HAb18G/CD147 as the target of antivirus antagonists and the obtained antivirus antagonists, there of. Patent Cooperation Treaty international patent PCT/CN03/00451. June 9, 2003.
20. Chen ZN, Qian AR, Shang P, et al. Targeting human hepatocellular carcinoma cell membrane antigen HAb18G/CD147 by its antagonistic peptides. J Tumor Marker Oncol **2003**; 18:5–18.
21. Chen ZN, Shang P, Li Y, Qian AR, Zhu P, Xing JL. HAb18G/CD147, its antagonist and application. PCT international patent WO02/094875. May 27, 2002.
22. Huang BC, Shang P, Qian AR, Wang XH, Shi GH, Chen ZN. Biopanning of antagonistic peptides against HAb18G/CD147 and their function of anti-hepatoma invasion. Chin J Oncol **2003**; 25:111–4.
23. Huang BC, Shang P, Qian AR, Chen ZN. Biopanning of hepatoma metastatic associated factor (HAb18G/CD147)'s peptide antagonist from a phage displayed random peptide library. J Tumor Marker Oncol **2001**; 16:290.
24. Qian AR, Shang P, Huang BC, Chen ZN, Luo ZQ, Zhang XD. A combined bioinformatic approach to analyzing the characteristics of antagonistic peptides against hepatocellular carcinoma marker HAb18G/CD147. J Tumor Marker Oncol **2003**; 18:29–38.
25. Chen ZN, Liu YF. Monoclonal antibody HAb18 to human hepatoma. Monoclonal Antibodies **1990**; 8:11–2.
26. Chen ZN, Xing JL, Zhang SH. Research and application of variable region of light and heavy chain of HAb18, the antihuman hepatoma monoclonal antibody. PCT international patent WO03/078469. March 17, 2003.
27. Chen ZN, Xing JL, Bian HJ, Mi L, Jiang JL. Application of cell engineering technology to the tumor immunotherapeutic drug: a review. Cell Biol Int **2001**; 25:1013–5.
28. Chen ZN, Liu YF, Jiang MD, Deng JL, Sui YF. Radiolocalization of human hepatoma with anti-human hepatoma monoclonal antibodies and its $F(ab')_2$ in tumor-bearing nude mice. Chin Med J **1989**; 69:566–8.
29. Liu Y, Chen ZN, Ji YY, et al. Localization of hepatocellular carcinoma with monoclonal antibodies. Chin Med J **1991**; 71:362–5.
30. Chen ZN, Liu YF, Sui YF, Yang JZ, Deng JL, Zhao YS. Significanc and application of anti-malignant hepatoma MAb HAb18 in radioimmunal diagnosis of human hepatocellular carcinoma. Chin J Oncol **1992**; 14: 9–12.
31. Bian HJ, Chen ZN, Deng JL. Direct technetium-99m labeling of anti-hepatoma monoclonal antibody fragment: a radioimmunoconjugate for hepatocellular carcinoma imaging. World J Gastroenterol **2000**; 6: 348–52.
32. Mi L, Chen ZN, Feng Q, Yu XL. Preparation of monoclonal antibody bivalent fragment and Fab fragment. Chinese patent 99115730.3. March 12, 1999.
33. Mi L, Li L, Feng Q, Yu XL. Technical methods of continuous perfusion culture hybridoma cells and CHO cells for production of monoclonal antibody. Chinese patent 01131736.1. September 29, 2001.
34. MacKenzie CR, Hirama T, Lee KK, Altman E, Young NM. Quantitative analysis of bacterial toxin affinit and specificit for glycolipid receptors by surface plasmon resonance. J Biol Chem **1997**; 272:5533–8.
35. Saphire AC, Bobardt MD, Gallay PA. Human immunodeficienc virus type 1 hijacks host cyclophilin A for its attachment to target cells. Immunol Res **2000**; 21:211–7.
36. Marra MA, Jones SJ, Astell CR, et al. The genome sequence of the SARS-associated coronavirus. Science **2003**; 300:1399–404.